PREPRINT

PERTANIKA JOURNALS

SCIENCE & TECHNOLOGY

Journal homepage: http://www.pertanika.upm.edu.my/

Mathematical Modelling of Scission Electrospun Polystyrene Fibre by Ultrasonication Scission

Cheryl Rinai Raja[1]*, Marini Sawawi[1], Shirley Johnathan Tanjong[1] and Nurliyana Truna[2]

[1]Faculty of Engineering, Universiti Malaysia Sarawak, Jalan Datuk Mohammad Musa, Kota Samarahan, 94300, Sarawak, Malaysia

[2]Pusat Pengajian Pra Universiti, Kampus Timur, Universiti Malaysia Sarawak, Kota Samarahan, 94300, Sarawak, Malaysia

ABSTRACT

This study investigates the effects of time and diameter on the final scission length of the electrospun polystyrene (PS) fibres, whereby the fibres were ultrasonicated for 1, 2, 3, 4, and 8 minutes. The ultrasonic probe stimulates bubble cavitation followed by bubble implosion as scission occurs. Factors affecting the scissionability of the electrospun PS fibres are primarily the diameter of the fibre and the sonication run time. The scission final fibre length range is approximately 23.7 µm to 1.1 µm. SEM images show that the fibre breaks into shorter lengths as sonication run time increases. Conversely, fibre diameter exhibits a positive relationship with fibre length. The model gives an R-squared value of 0.44 and 0.59 for linear and non-linear regression, thus suggesting that the non-linear model provides a better fit for the data. The validation of the model is achieved by conducting a hypothesis test. Through hypothesis testing, the mean of the experimental average final length value and the predicted average fibre length from the regression model were not significant, indicating that the model can generally predict a relatively accurate average final fibre length value. The model derived from this study enables researchers to estimate the time required to sonicate the PS fibre (with a specific diameter) to achieve the short fibre length needed in their application. As research progresses, refining the model and incorporating additional parameters will be essential to ensure the broad reliability and applicability of these models across a variety of practical contexts.

Keywords: Electrospinning, mathematical modelling, polystyrene, regression, scission, ultrasonication

ARTICLE INFO

Article history:
Received: 27 June 2023
Accepted: 20 November 2023
Published: 01 April 2024

DOI: https://doi.org/10.47836/pjst.32.3.06

E-mail addresses:
cheryl.raja@gmail.com (Cheryl Rinai Raja)
smarini@unimas.my (Marini Sawawi)
jtshirley@unimas.my (Shirley Johnathan Tanjong)
tliyana@unimas.my (Nurliyana Truna)
* Corresponding author

ISSN: 0128-7680
e-ISSN: 2231-8526

INTRODUCTION

The process of using electrostatic forces to produce synthetic fibres with diameters and lengths of the submicron scale (Doshi & Reneker, 1995) has piqued the interest of researchers over the past century, especially due to its wide range of applications. In this procedure, referred to as electrospinning, a high-voltage source is used to induce a certain polarity of charge into a polymer solution or melt, which is subsequently accelerated toward a collector of a different polarity (Subbiah et al., 2005). However, the electrospinning process is limited to producing only long, thin, continuous fibres with a limited range of applications compared to that of discontinuous, short electrospun fibres. Unlike the length, the diameter, as well as other characteristics of the electrospun fibre, can be manipulated by optimising the electrospinning parameters (Valizadeh & Farkhani, 2014).

The tailorable parameters include the type of solvents, solution concentration, collection rate, gap distance, applied voltage, drop height, and fibre orientation. These processing parameters will highly influence the characteristics of the electrospun nanofibers, such as fibre diameter (Khanlou et al., 2015), morphology (Megelski et al., 2002), porosity (Baker et al., 2008), mechanical properties (O'Connor et al., 2021), chemical composition (Lima et al., 2020) and uniformity (Zhang et al., 2021). Such characteristics require optimising these parameters to maximise their performance for specific applications. For instance, Zhang et al. (2021) reported that 1000rpm was the optimal rotational speed in creating electrospun PCL fibres with aligned topography, which would serve as a promising candidate for nerve guidance conduits (NGCs) and other tissue engineering applications. Furthermore, different solvents have also been reported by Maleki et al. (2013), where electrospun PLLA yarns produced had the highest tensile strength as well as Young's modulus and a higher elongation at break when using chloroform and dichloromethane respectively. However, producing short continuous fibres through electrospinning is impossible just by adjusting the parameters.

A secondary process is needed to produce the desired discontinuous short fibres (Luo et al., 2011). Such secondary process includes mechanical cutting (Thieme et al., 2011), ultra-violet (UV) cutting (Li et al., 2010), microtome cutting (Oksman et al., 2009), micro cutting under liquid nitrogen (Magill & Gunning, 1969), cryogenic milling (Morkavuk et al., 2018), ball milling (Hrabalova et al., 2011) as some of the less popular scission methods. One method which has been widely reported for the scission of carbon nanotubes or even electrospun nanofibers is by means of ultrasonication (Chew et al., 2011; Hennrich et al., 2007; Liu et al., 2017; Niemczyk-Soczynska et al., 2021; Pagani et al., 2012).

Ultrasonication is widely used in the dispersion of solutes, especially carbon nanotubes (Ahir et al., 2008; Kharissova & Kharisov, 2017). Studies employing the ultrasonication technique for exfoliating carbon nanotubes (CNTs) have reported scission as an unwanted

side effect (Stegen, 2014), which later garnered more attention from researchers. This technique allows for scission of the carbon nanotubes through the mechanism of bubble cavitation and implosion. When ultrasound is used to insonify a liquid medium, a sequence of compression and rarefaction cycles results, creating regions with high and low local pressures (Lucas et al., 2009). Existing gas nuclei expand as a result of the dissolved gas's desorption to create cavitation bubbles. High local temperatures and pressures are caused by these transient cavities, which first grow before rapidly collapsing in subsequent compression cycles. When cavitation bubbles collide close to an interface, liquid jets are expelled, causing an impact with a mechanical effect on the surrounding material (Ando, 1991; Sander et al., 2014; Tsochatzidis et al., 2001). The van der Waals forces and other nonbonding interactions between the nanofibers, which are essentially bound to one other through nonbonding interactions, can be broken by said impact. This approach offers a practical, adaptable, and eco-friendly fabrication technique for the large-scale production of short nanofibers.

Discontinuous short electrospun fibres are versatile and can be used for various applications such as scaffolds (Li et al., 2006) or carrier matrices in tissue engineering (Lannutti et al., 2007), drug delivery (Zeng et al., 2003), wound healing (Casper et al., 2005), filtration systems (Bortolassi et al., 2019), micro-electronic (Luzio et al., 2014) applications, fibre reinforcement (Chen et al., 2011) and many more (Bhardwaj & Kundu, 2010; Jiang et al., 2018; Schiffman & Schauer, 2008). Therefore, it is important to study the process of producing these electrospun short fibres.

Several works of literature discuss the theoretical process of the scission caused by the shear stress and strain forces imposed on the carbon nanotubes (CNTs) by the imploding bubble in ultrasonication (Ahir et al., 2008; Heller et al., 2004; Hennrich et al., 2007; Huang et al., 2009; Pagani et al., 2012; Stegen, 2014). While some of these were derived with comparison to the scission modelling of polymer fibres whereby the fractures were deemed non-random as the point of scission typically occurs at the centre of mass (Kuijpers et al., 2004; Price & Smith, 1991), another study have discussed the degradation of polymer fibres with respect to time (Van Der Hoff & Glynn, 1974). Through this research, very few have addressed the simultaneous effects of several variables as predictors for the final fibre length. A mathematical model that predicts the final fibre length and predictor variables will be useful to pre-determine the exact input parameters to achieve the desired length. Hence, this research aims to predict the average final length of scission electrospun polystyrene (PS) nanofiber by ultrasonication while considering the scission time and diameter (the predictor variables) of the polymer fibre. A multiple regression model could provide a foundation for further research, potentially paving the way for precise control of submicron-length fibres on a large scale.

METHOD AND MATERIALS

Electrospinning

The parameters of the electrospinning and ultrasonication process to produce the short electrospun fibres were optimised from the previous works (Sawawi et al., 2013). The electrospinning process was conducted using an electrospinner built in the laboratory, which used a high voltage supply from Gamma High Voltage Research (USA), whilst the syringe pump was from Razel Scientific Instruments, Inc. (USA).

The PS fibres were produced by varying the concentration to obtain three sizes of fibre diameter to investigate the effect of fibre diameter on ultrasonication scission. The thinner PS fibres were electrospun at 8 wt/v%, whilst the larger fibre diameter was achieved when electrospun was at 16 wt/v%. All the fibres for these comparative purposes were electrospun in the same solvent solution, a mixture of chloroform and DMF (1:1) with 1 mM DTAB at the same speed of rotating mandrel of 6.8 m/s surface velocity. After collection, the non-woven web was stored in a desiccator under vacuum prior to further use. The other electrospinning parameters were kept the same: a 1.6 mL/hr feed rate, 20 kV accelerating voltage, 6 cm working distance and 18G gauged needle. The optimum voltage for 8 wt/v% is 15 kV. The electrospinning parameters are listed in Table 1.

Table 1
Electrospinning parameters (Sawawi et al., 2013)

Material	Solvent	Concentration (%)(w/v)	Feed rate (ml/hr)	Voltage (+kV)	Needle size (G)	Working distance (cm)	Mandrel speed (m/s)
PS	Chloroform + DMF (1 mM DTAB)	8	1.6	15	18	6	**6.3**
PS	Chloroform + DMF (1 mM DTAB)	12	1.6	20	18	6	**6.3**
PS	Chloroform + DMF (1 mM DTAB)	16	1.6	20	18	6	**6.3**

Ultrasonication

In the scissioning process, the electrospun webs were peeled off the collection plate, and a 1 cm^2 area was cut with a sharp knife before being placed randomly in a glass vial (25 mm in diameter) containing 15 mL of MiliQ water. The sonication was carried out using a Vibracell 750W (Sonics & Materials, Inc, USA) sonicator probe with a probe diameter of 13 mm and a working frequency of 20 kHz. The probe was positioned ca. 1 cm from the bottom of the vial. The processing parameters varied, such as total run time, amplitude percentage, and lapsed ON/OFF time. The water used for this study was at ambient

conditions. In general, ultrasonication was conducted in a beaker cooled by water-ice slurry to maintain the processing temperatures below 30°C since ongoing sonication raises the solvent temperature, even when using ON/OFF pulsed exposure.

After completion of the ultrasonic treatment, short fibres in the solvent suspension were placed on a scanning electron microscope (SEM) stub, which was covered with double-sided carbon tape to allow adhesion to the stub. Prior to SEM imaging, the sample was dried overnight in the fumehood followed by 2 hr in a vacuum oven at 60°C and platinum-coated at 1 nm thickness with a sputter coater, Cressington 208HR, (UK).

Mathematical Modelling

In this study, the mathematical model is designed through model assumptions that sonication run time and the diameter of the electrospun fibre influence the final fibre length. The relationship between the sonication run time, the diameter and the limiting length is studied through the regression analysis. A general multiple linear regression model (Zain et al., 2012) is expressed as Equation 1:

$$y = b_0 + b_1 x_1 + b_2 x_2 + b_3 x_3 + \cdots b_n x_n \quad [1]$$

whereby y is the dependent variable, b_o is the intercept parameter, $b_1, b_2, b_3 \ldots, b_n$ are the slope parameters, and x_n is the independent variable. This model is suitable for describing a linear relationship between the independent and dependent variables. In this model, the data used for the analysis was based on the quantified experimental data of the electrospun aligned PS 8wt% and 16wt% to generate a model covering the range of diameter, d from 240 μm to 930 μm respectively. The regression mathematical models developed in this study are produced using the Minitab and Microsoft Excel software. Multiple linear and non-linear regression analysis was used to develop the mathematical model, and the two models were compared. Data for the ultrasonicated electrospun 12wt% PS fibre was used to conduct the hypothesis testing. Table 2 summarises the descriptive statistics of the data obtained from the experiment used to construct the model.

Table 2
Summary of experimental data statistics

Variable	N	N*	Mean	SE Mean	StDev	Minimum	Q1	Median	Q3	Maximum
Y	406	0	6.820	0.386	7.780	0.450	2.083	3.758	8.241	46.666
X1	406	0	585.0	17.1	345.4	240.0	240.0	585.0	930.0	930.0
X2	406	0	4.254	0.113	2.285	2.000	2.000	3.500	8.000	8.000

CHARACTERISATION

Scanning Electron Microscopy

Scanning electron microscopy (SEM) is used to study the morphology and microstructure of a solid surface, which is important in understanding the structure-property relationship of a material. In this method, the sample surface is scanned by a high-energy electron beam where the incident electrons interact with the specimen atoms and cause extensive scattering. The SEM was conducted using a Scanning Electron Microscope (JEOL840A JEOL Ltd, Japan). The short fibre samples were dried overnight in the fumehood, followed by heating at 60°C in a vacuum oven for 2 hr prior to platinum coating of the sample (1 nm thickness) using a sputter coater (Cressington 208HR, UK).

RESULTS AND DISCUSSION

Scanning Electron Microscopy

SEM was performed on the as-spun PS fibre before and after ultrasonication to compare the surface morphology and quantify the average fibre length of the short fibres. Figure 1 shows the electrospun fibres before and after sonication for what we define in this work as the "minimum sonication time," which was found to be 1 minute. This minimum sonication time is defined as the first time that the web was visually observed to significantly fragment, which was found. The sonicated fibres are of 732 ± 312 nm diameters in aligned orientation having 12wt/v%.

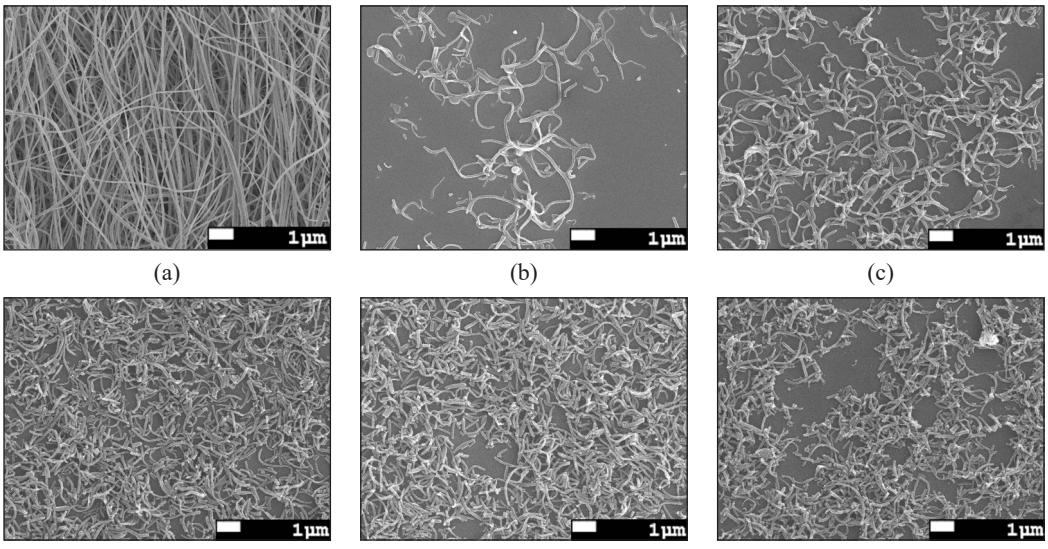

(a) (b) (c)

(d) (e) (f)

Figure 1. SEM images of electrospun PS fibres with aligned orientation under various sonication times at ×1.5k magnification: (a) as-spun PS fibre; (b) 1 minute; (c) 2 minutes; (d) 3 minutes; (e) 4 minutes; and (f) 8 minutes

Figure 1(a) is the as-spun un-ultrasonicated electrospun PS fibre which appears as a continuous web or mesh of fibres when compared to the ultrasonicated fibres in Figures 1(b), 1(c), 1(d), 1(e) and 1(f). In this study, the fibres are found to be scissioned with a minimum time of 1 minute. However, comparing Figures 1(b) to 1(c), 1(d), 1(e) and 1(f), the discontinuous fibres are still long and do not have enough discrete discontinuous fibres to be quantified. Fibres sonicated at 2, 3, 4 and 8 minutes show discrete, discontinuous fibres where the end-to-end of the singular fibres can be observed. The average final fibre length reduces as sonication run time increases, with the longest length being 5.63±4.38 µm at 2 minutes and the shortest average final length of 2.17±0.75 µm at 8 minutes (Table 3). Factors affecting the scissionability of the fibres include the diameter and time.

Figure 2 compares the average final fibre length of ultrasonicated electrospun PS fibres with different diameters. The concentration of the polymer influences the variance of diameter. The 8wt/v%, 12wt/v% and 16wt/v% have diameters of d_1 =240 ± 70 nm, d_2 = 732 ± 312 nm and d_3 = 930 ± 290 nm respectively (images not shown here). It can be observed in the graph that the electrospun fibre with the largest diameter, d_3 (16wt/v%), has a longer final fibre length after sonication. In contrast, the shortest length is achieved by the fibre with the smallest diameter, d_1 (8wt/v%). Regardless of diameter size, a negative trend can

Table 3
Average final aligned PS fibre length after ultrasonication

Diameter, d (nm)	**732 ± 312**	**732 ± 312**	**732 ± 312**	**732 ± 312**
Time, t (minutes)	2	3	4	8
Average final fibre length, L_{avg} (microns)	5.625 ± 4.384	3.922 ± 2.092	2.915 ± 0.999	2.174 ± 0.749

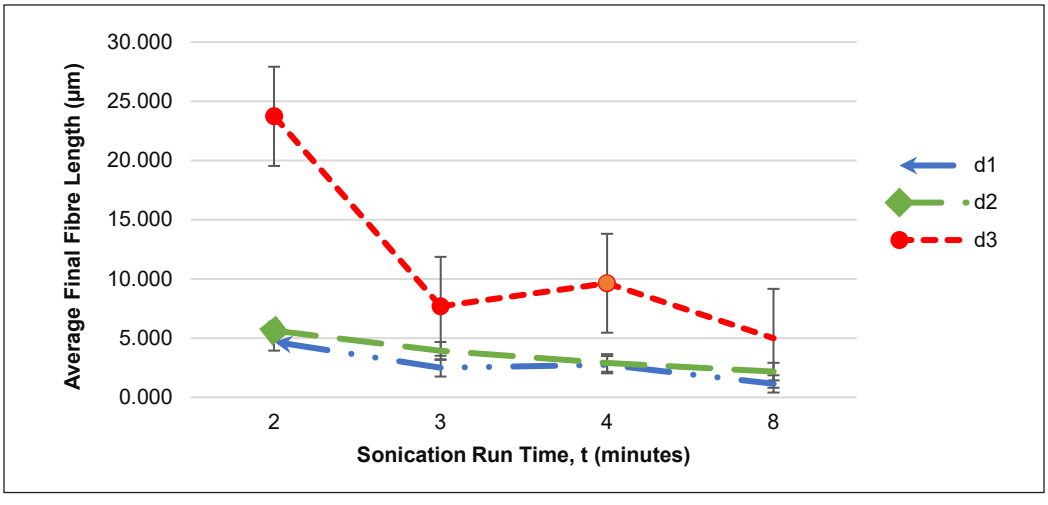

Figure 2. Average final fibre length against the sonication run time of electrospun PS fibres with different diameters

be observed from the graph, which also concludes the negative relationship between the sonication run time and final length. The opposite is implied for the relationship between the diameter and the average final fibre length.

Multiple Regression Modelling

Equation 2 shows the multiple linear regression model obtained using the Minitab software.

$$L_{avg} = 5.349 + 0.012125d - 1.322t \quad [2]$$

The linear regression model analysis resulted in an R^2 value of 0.44 and p<0.001, which indicates that the relationship between x_1 (diameter, d) and x_2 (time, t) and y (average fibre length, L_{avg}) is statistically significant. This model may not accurately represent the relationship between the effects of time and diameter on the final fibre length; therefore, as a comparison, a non-linear regression model was also generated using the Minitab software, resulting in Equation 3.

$$L_{avg} = 14.30 + 0.02278d - 7.404t + 0.7257t^2 - 0.002500dt \quad [3]$$

where Y is the average final length, X_1 is the diameter(μm), and X_2 is the sonication time(min). Equation 3 represents a non-linear regression model of the relationship between L_{avg}, d and t. According to the analysis, the model R^2 value is 0.5989. It means that 59.89% of the variation in the response variable can be explained by the predictor variables (d and t). The relationship between the variables in this model is statistically significant with $p < 0.001$, less than 0.05. It means that a relationship exists between the response and predictor variables. According to Viloria et al. (2016), if the R-squared value is above 80%, it indicates that the independent variables are enough to explain the relationship to the dependent variable. However, for the models in this study, the parameters may not be enough to explain the behaviour of the fibre scission by ultrasonication given that the R^2 is less than 80% because ultrasonication is a random process in terms of positions of bubble cavitation, which causes the scission of the fibre. It can also be explained by the high standard deviation obtained from sonication, which shows the variability of the data. However, at a higher sonication time, the R^2 value is significantly higher at 65.9% since a longer sonication run time will produce shorter fibres up to a point where it stabilises.

Referring to Equations 2 and 3, the coefficient of the variable for time, t, shows a negative value, which indicates that as the sonication run time increases, the final fibre length decreases. In contrast, the positive value for the diameter variable, d, suggests that the average final length increases as the diameter increases. This non-linear regression model concludes that it better fits the data with the trend aligned with the initial model

assumptions. Although regression analysis can help identify the type and strength of correlations, it is unable to differentiate between indirect and direct effects or consider the complex interaction between cause and effect.

Average Length vs Model Length

The mathematical model in Equation 3 was verified using the 12wt/v% of PS concentration, in which the data is tabulated in Table 4. The graphical output is shown in Figure 3; the difference in values between the model and the actual average final fibre length at 2 minutes is large, whereby even the maximum final length value does not overlap with the modelled value. However, it should be noted that in the sonication experiment, the fibre length varies significantly. For example, when calculating the maximum length for 2 minutes of sonication time, the length was 10 µm, about 50% of the estimated fibre length, using Equation 3. It is also true for other sonication times. As the sonication increases (such as at 8 minutes), the maximum fibre length was found to be 2.92 µm (about 20% difference). The average final fibre length after 8 minutes of sonication is 2.17±0.749 µm, and the modelled fibre length is ~3.54 µm. If the maximum value is 2.92 µm, it is closer to the modelled length. The difference can be neglected as it is ~0.62 µm. Furthermore, as the sonication run-time approaches 8 minutes, the model has a similar trend to the actual data.

Table 4
Actual final length and predicted final length using the model

Time	**2**	**3**	**4**	**8**
Mathematical Model (Equation 3)	15.37	9.77	5.62	3.54
Actual experiment average final fibre length L_{avg}	5.63 ± 4.384	3.69 ± 2.092	2.86 ± 0.999	2.17 ± 0.749

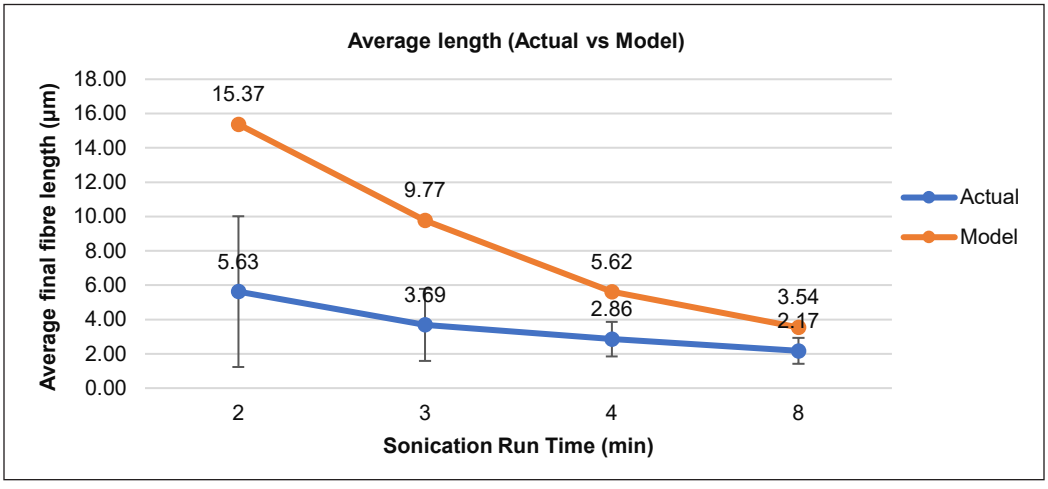

Figure 3. Graph of average final fibre length based on experiment (actual) and prediction (model)

To validate the model, a 2-sample independent t-test was conducted. It was highlighted that there is no significant difference ($p>0.05$) between the mean of the experimental value and the average fibre length predicted from the regression model (Figure 4). It indicates that the model describes the fibre length generally accurately. This test concludes that it is possible to develop the model for the scission of electrospun fibres to determine the final fibre length given the diameter and sonication run time. However, precaution needs to be taken whereby the fibre length can vary from 50% to 20%. The fibre length that resulted from this process is in tens-micron size, which does not make a significant difference when only 2-5-micron length differs.

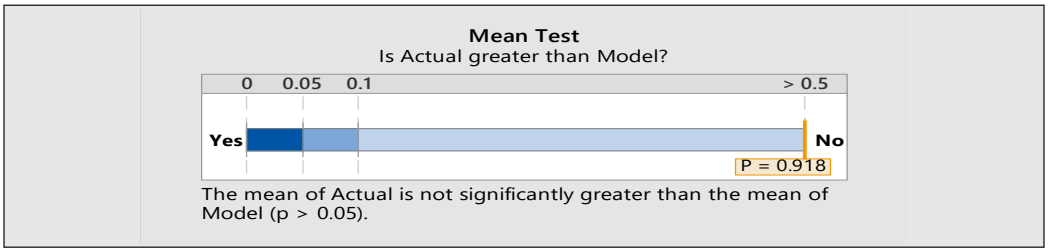

Figure 4. 2-sample independent t-test

Limitations and Recommendations

Though the model does show a relation between the variables, it does have a few notable limitations, such as its reliance on a specific experimental setting. Since this model is based on electrospun fibres from the previous study, the variables involved are limited, thus making the model only applicable to the difference in diameter for PS. It limits the model's generalizability, which does not allow it to fully capture the complexity of all possible scenarios and variations in the scissioning process. Furthermore, the model shows equipment dependency, which can only be used for PS electrospun nanofibers being sonicated using specific equipment with specific parameters. Variations in equipment specifications or configurations may not be accounted for, potentially restricting the model's applicability in a broader range of experimental setups. The generated model is also based on only one type of material, which limits its application in studying the scission effects of other materials as different materials have different characteristics.

In future research, the model's robustness can be improved by including additional parameters, such as the variables related to both the sonication process and the type of materials, which allows a better understanding of their effects on one another. Each material has distinct characteristics which would facilitate a more inclusive analysis. Including diverse materials would also enhance the model's reliability by using it for validation to increase the its accuracy in a broader context. Furthermore, the model can be improved by considering the inherent variability in real-world processes, such as a safety factor, to

account for the unpredictability of certain experimental conditions. Conducting sensitivity analysis can also help in providing insight into the model's responsiveness to parameter variations. It would help identify critical factors that significantly impact the outcomes, guiding the experimental efforts and model refinement.

CONCLUSION

This study has applied a regression analysis to produce a model equation of ultrasonicated electrospun PS fibres. It is found that a quadratic multiple regression model better fits the data as the correlation between the diameter and time with respect to the final fibre length do not linearly respond to one another. As observed, the average final fibre length decreases when the sonication run time increases. The opposite is concluded for the relationship between the diameter and the final fibre length; as the diameter increases, the fibre length also increases. The quadratic regression model is statistically significant, whereby the model can explain 59.89% of the data. Furthermore, through hypothesis testing, the mean of the experimental value and the average fibre length predicted from the regression model are not significant, which indicates that the model can generally predict a relatively accurate average final fibre length value. While acknowledging the model's limitations, such as equipment and material dependencies, it provides a foundation for further research. In the future, the mathematical model might be more refined to provide an exact length value to ease the production of these submicron-length fibres on a large scale. More variables can be added to the modelling to produce a higher R^2 value feasible for large-scale production. The ability to create short, discontinuous electrospun fibres through ultrasonication holds tremendous promise for a wide range of applications, including tissue engineering, drug delivery, filtration systems, and more. As we move forward, refining the model and incorporating additional parameters to enhance its robustness is imperative. Exploring the effects of different materials, conducting sensitivity analyses, and accounting for real-world variability are essential steps to ensure the reliability and broad applicability of these models. Ultimately, this research contributes to our understanding of electrospinning and paves the way for more precise control of fibre properties in various practical contexts.

ACKNOWLEDGEMENTS

The authors thank the Ministry of Higher Education, Malaysia, Fundamental Research Grant Scheme (FRGS/1/2020/TK0/UNIMAS/02/12 and Universiti Malaysia Sarawak (F02/FRGS/1999/2020) for supporting this work**.**

REFERENCES

Ahir, S. V., Huang, Y. Y., & Terentjev, E. M. (2008). Polymers with aligned carbon nanotubes: Active composite materials. *Polymer*, *49*(18), 3841–3854. https://doi.org/10.1016/j.polymer.2008.05.005

Ando, T. (1991). Ultrasonic organic synthesis involving non-metal solids. *Advances in Sonochemistry*, *2*, 211-251.

Baker, B. M., Gee, A. O., Metter, R. B., Nathan, A. S., Marklein, R. A., Burdick, J. A., & Mauck, R. L. (2008). The potential to improve cell infiltration in composite fiber-aligned electrospun scaffolds by the selective removal of sacrificial fibers. *Biomaterials*, *29*(15), 2348–2358. https://doi.org/10.1016/J.BIOMATERIALS.2008.01.032

Bhardwaj, N., & Kundu, S. C. (2010). Electrospinning: A fascinating fiber fabrication technique. *Biotechnology Advances*, *28*(3), 325–347. https://doi.org/10.1016/j.biotechadv.2010.01.004

Bortolassi, A. C. C., Nagarajan, S., de Araújo Lima, B., Guerra, V. G., Aguiar, M. L., Huon, V., Soussan, L., Cornu, D., Miele, P., & Bechelany, M. (2019). Efficient nanoparticles removal and bactericidal action of electrospun nanofibers membranes for air filtration. *Materials Science and Engineering C*, *102*, 718–729. https://doi.org/10.1016/j.msec.2019.04.094

Casper, C. L., Yamaguchi, N., Kiick, K. L., & Rabolt, J. F. (2005). Functionalizing electrospun fibers with biologically relevant macromolecules. *Biomacromolecules*, *6*(4), 1998–2007. https://doi.org/10.1021/bm050007e

Chen, D., Wang, R., Tjiu, W. W., & Liu, T. (2011). High performance polyimide composite films prepared by homogeneity reinforcement of electrospun nanofibers. *Composites Science and Technology*, *71*(13), 1556–1562. https://doi.org/10.1016/j.compscitech.2011.06.013

Chew, H. B., Moon, M. W., Lee, K. R., & Kim, K. S. (2011). Compressive dynamic scission of carbon nanotubes under sonication: Fracture by atomic ejection. *Proceedings of the Royal Society A: Mathematical, Physical and Engineering Sciences*, *467*(2129), 1270–1289. https://doi.org/10.1098/rspa.2010.0495

Doshi, J., & Reneker, D. H. (1995). Electrospinning process and applications of electrospun fibers. *Electrospinning Process and Applications of Electrospun Fibres*, *3*(2-3), 151–160. https://doi.org/10.1109/ias.1993.299067

Heller, D. A., Mayrhofer, R. M., Baik, S., Grinkova, Y. V., Usrey, M. L., & Strano, M. S. (2004). Concomitant length and diameter separation of single-walled carbon nanotubes. *Journal of the American Chemical Society*, *126*(44), 14567–14573. https://doi.org/10.1021/ja046450z

Hennrich, F., Krupke, R., Arnold, K., Stütz, J. A. R., Lebedkin, S., Koch, T., Schimmel, T., & Kappes, M. M. (2007). The mechanism of cavitation-induced scission of single-walled carbon nanotubes. *Journal of Physical Chemistry B*, *111*(8), 1932–1937. https://doi.org/10.1021/jp065262n

Hrabalova, M., Schwanninger, M., Wimmer, R., Gregorova, A., Zimmermann, T., & Mundigler, N. (2011). Fibrillation of flax and wheat straw cellulose: Effects on thermal, morphological, and viscoelastic properties of poly(vinylalcohol)/fibre composites. *BioResources*, *6*(2), 1631–1647. https://doi.org/10.15376/biores.6.2.1631-1647

Huang, Y. Y., Knowles, T. P. J., & Terentjev, E. M. (2009). Strength of nanotubes, filaments, and nanowires from sonication-onduced scission. *Advanced Materials*, *21*(38–39), 3945–3948. https://doi.org/10.1002/adma.200900498

Jiang, S., Chen, Y., Duan, G., Mei, C., Greiner, A., & Agarwal, S. (2018). Electrospun nanofiber reinforced composites: A review. *Polymer Chemistry*, *9*(20), 2685–2720. https://doi.org/10.1039/c8py00378e

Khanlou, H. M., Ang, B. C., Talebian, S., Barzani, M. M., Silakhori, M., & Fauzi, H. (2015). Multi-response analysis in the processing of poly (methyl methacrylate) nano-fibres membrane by electrospinning based on response surface methodology: Fibre diameter and bead formation. *Measurement*, *65*, 193–206. https://doi.org/10.1016/j.measurement.2015.01.014

Kharissova, O. V., & Kharisov, B. I. (2017). *Solubilization and dispersion of carbon nanotubes*. Springer. https://doi.org/10.1007/978-3-319-62950-6

Kuijpers, M. W. A., Iedema, P. D., Kemmere, M. F., & Keurentjes, J. T. F. (2004). The mechanism of cavitation-induced polymer scission; experimental and computational verification. *Polymer*, *45*(19), 6461–6467. https://doi.org/10.1016/j.polymer.2004.06.051

Lannutti, J., Reneker, D., Ma, T., Tomasko, D., & Farson, D. (2007). Electrospinning for tissue engineering scaffolds. *Materials Science and Engineering C*, *27*(3), 504–509. https://doi.org/10.1016/j.msec.2006.05.019

Li, M., Mondrinos, M. J., Chen, X., Gandhi, M. R., Ko, F. K., & Lelkes, P. I. (2006). Co-electrospun poly(lactide-co-glycolide), gelatin, and elastin blends for tissue engineering scaffolds. *Journal of Biomedical Materials Research - Part A*, *79*(4), 963–973. https://doi.org/10.1002/jbm.a.30833

Li, Z. L., Zheng, H. Y., Lim, G. C., Chu, P. L., & Li, L. (2010). Study on UV laser machining quality of carbon fibre reinforced composites. *Composites Part A: Applied Science and Manufacturing*, *41*(10), 1403–1408. https://doi.org/10.1016/j.compositesa.2010.05.017

Lima, L. L., Bierhalz, A. C. K., & Moraes, Â. M. (2020). Influence of the chemical composition and structure design of electrospun matrices on the release kinetics of Aloe vera extract rich in aloin. *Polymer Degradation and Stability*, *179*, 109233. https://doi.org/10.1016/j.polymdegradstab.2020.109233

Liu, C., Shi, H., Yang, H., Yan, S., Luan, S., Li, Y., Teng, M., Khan, A. F., & Yin, J. (2017). Fabrication of antibacterial electrospun nanofibers with vancomycin-carbon nanotube via ultrasonication assistance. *Materials and Design*, *120*, 128–134. https://doi.org/10.1016/j.matdes.2017.02.008

Lucas, A., Zakri, C., Maugey, M., Pasquali, M., Schoot, P. V. D., & Poulin, P. (2009). Kinetics of nanotube and microfiber scission under sonication. *Journal of Physical Chemistry C*, *113*(48), 20599–20605. https://doi.org/10.1021/jp906296y

Luo, C. J., Stride, E., Stoyanov, S., Pelan, E., & Edirisinghe, M. (2011). Electrospinning short polymer micro-fibres with average aspect ratios in the range of 10-200. *Journal of Polymer Research*, *18*(6), 2515–2522. https://doi.org/10.1007/s10965-011-9667-6

Luzio, A., Canesi, E. V., Bertarelli, C., & Caironi, M. (2014). Electrospun polymer fibers for electronic applications. *Materials, 7*(2), 906-947. https://doi.org/10.3390/ma7020906

Magill, H., & Gunning, B. (1969). A simple microtome capable of cutting sections of plastic-embedded material down to 1 µm in thickness. *Journal of Microscopy*, *89*(2), 217–223. https://doi.org/10.1111/j.1365-2818.1969.tb00667.x

Maleki, H., Gharehaghaji, A. A., Moroni, L., & Dijkstra, P. J. (2013). Influence of the solvent type on the morphology and mechanical properties of electrospun PLLA yarns. *Biofabrication*, *5*(3), Article 035014. https://doi.org/10.1088/1758-5082/5/3/035014

Megelski, S., Stephens, J. S., Bruce Chase, D., & Rabolt, J. F. (2002). Micro- and nanostructured surface morphology on electrospun polymer fibers. *Macromolecules*, *35*(22), 8456–8466. https://doi.org/10.1021/ma020444a

Morkavuk, S., Köklü, U., Bağcı, M., & Gemi, L. (2018). Cryogenic machining of carbon fiber reinforced plastic (CFRP) composites and the effects of cryogenic treatment on tensile properties: A comparative study. *Composites Part B: Engineering*, *147*, 1–11. https://doi.org/10.1016/j.compositesb.2018.04.024

Niemczyk-Soczynska, B., Dulnik, J., Jeznach, O., Kolbuk, D., & Sajkiewicz, P. (2021). Shortening of electrospun PLLA fibers by ultrasonication. *Micron*, *145*, Article 103066. https://doi.org/10.1016/j.micron.2021.103066

O'Connor, R. A., Cahill, P. A., & McGuinness, G. B. (2021). Effect of electrospinning parameters on the mechanical and morphological characteristics of small diameter PCL tissue engineered blood vessel scaffolds having distinct micro and nano fibre populations – A DOE approach. *Polymer Testing*, *96*, Article 107119. https://doi.org/10.1016/j.polymertesting.2021.107119

Oksman, K., Mathew, A. P., Långström, R., Nyström, B., & Joseph, K. (2009). The influence of fibre microstructure on fibre breakage and mechanical properties of natural fibre reinforced polypropylene. *Composites Science and Technology*, *69*(11–12), 1847–1853. https://doi.org/10.1016/j.compscitech.2009.03.020

Pagani, G., Green, M. J., Poulin, P., & Pasquali, M. (2012). Competing mechanisms and scaling laws for carbon nanotube scission by ultrasonication. *Proceedings of the National Academy of Sciences of the United States of America*, *109*(29), 11599–11604. https://doi.org/10.1073/pnas.1200013109

Price, G. J., & Smith, P. F. (1991). Ultrasonic degradation of polymer solutions. 1. Polystyrene revisited. *Polymer International*, *24*(3), 159–164. https://doi.org/10.1002/pi.4990240306

Sander, J. R. G., Zeiger, B. W., & Suslick, K. S. (2014). Sonocrystallization and sonofragmentation. *Ultrasonics Sonochemistry*, *21*(6), 1908–1915. https://doi.org/10.1016/j.ultsonch.2014.02.005

Sawawi, M., Wang, T. Y., Nisbet, D. R., & Simon, G. P. (2013). Scission of electrospun polymer fibres by ultrasonication. *Polymer*, *54*(16), 4237–4252. https://doi.org/10.1016/j.polymer.2013.05.060

Schiffman, J. D., & Schauer, C. L. (2008). A review: Electrospinning of biopolymer nanofibers and their applications. *Polymer Reviews*, *48*(2), 317–352. https://doi.org/10.1080/15583720802022182

Stegen, J. (2014). Mechanics of carbon nanotube scission under sonication. *Journal of Chemical Physics*, *140*(24), Article 244908. https://doi.org/10.1063/1.4884823

Subbiah, T., Bhat, G. S., Tock, R. W., Parameswaran, S., & Ramkumar, S. S. (2005). Electrospinning of nanofibers. *Journal of Applied Polymer Science*, *96*(2), 557–569. https://doi.org/10.1002/app.21481

Thieme, M., Agarwal, S., Wendorff, J. H., & Greiner, A. (2011). Electrospinning and cutting of ultrafine bioerodible poly(lactide-co-ethylene oxide) tri- and multiblock copolymer fibers for inhalation applications. *Polymers for Advanced Technologies*, *22*(9), 1335–1344. https://doi.org/10.1002/pat.1617

Tsochatzidis, N. A., Guiraud, P., Wilhelm, A. M., & Delmas, H. (2001). Determination of velocity, size and concentration of ultrasonic cavitation bubbles by the phase-Doppler technique. *Chemical Engineering Science*, *56*(5), 1831–1840. https://doi.org/10.1016/S0009-2509(00)00460-7

Valizadeh, A., & Farkhani, S. M. (2014). Electrospinning and electrospun nanofibres. *IET Nanobiotechnology*, *8*(2), 83–92. https://doi.org/10.1049/iet-nbt.2012.0040

Van Der Hoff, B. M. E., & Glynn, P. A. R. (1974). The Rate of degradation by ultrasonation of polystyrene in solution. *Journal of Macromolecular Science: Part A - Chemistry*, *8*(2), 429–449. https://doi.org/10.1080/00222337408065839

Viloria, A., Urbina, M. C., Rodríguez, L. G., & Muñoz, A. P. (2016). Predicting of behavior of escherichia coli resistance to Imipenem and Meropenem, using a simple mathematical model regression. *Indian Journal of Science and Technology*, *9*(46), 1-5. https://doi.org/10.17485/ijst/2016/v9i46/107379

Zain, A. M., Haron, H., Qasem, S. N., & Sharif, S. (2012). Regression and ANN models for estimating minimum value of machining performance. *Applied Mathematical Modelling*, *36*(4), 1477–1492. https://doi.org/10.1016/j.apm.2011.09.035

Zeng, J., Xu, X., Chen, X., Liang, Q., Bian, X., Yang, L., & Jing, X. (2003). Biodegradable electrospun fibers for drug delivery. *Journal of Controlled Release*, *92*(3), 227–231. https://doi.org/10.1016/S0168-3659(03)00372-9

Zhang, J., Zhang, X., Wang, C., Li, F., Qiao, Z., Zeng, L., Wang, Z., Liu, H., Ding, J., & Yang, H. (2021). Conductive composite fiber with optimized alignment guides neural regeneration under electrical stimulation. *Advanced Healthcare Materials*, *10*(3), Article 2000604. https://doi.org/10.1002/adhm.202000604